International Journal of Applied Mathematics
Volume 38 No. 11s, 2025
ISSN: 1311-1728 (printed version); ISSN: 1314-8060 (on-line version)

ENHANCED MASK REGIONAL BASED CONVOLUTIONAL NEURAL NETWORK USED FOR DETECTING PERCENTAGE OF MAIZE LEAF DAMAGE

V. Arockia Mary Epsy[1], Dr. P. Radha[2]

epsy1984@gmail.com[1], radhamuthu.cbe@gmail.com [2]

[1]Ph.D. Research Scholar, PG & Research Department of Computer Science, Government Arts College,Coimbatore-18.

[2]Associate Professor, PG & Research Department of Information Technology, Government Arts College,Coimbatore-18.

Abstract

In this work, an Enhanced Mask R-CNN-based segmentation approach combined with an Adaptive Median Neural Network (AMNN) for denoising is provided for accurate detection and quantification of pest-affected maize leaf regions. Pest infestation is one of the major challenges in maize crop production, resulting in great yield losses. Four major pests, namely armyworms, aphids, grasshoppers, and beetles, are analyzed on datasets from Roboflow and Mendeley. This Paper using 4 datasets for finding the maize leaf affected percentage. From the segmentation results, shows that the highest percentage of leaf damage was caused by armyworm followed by aphids, grasshoppers, and beetles. The exact quantification of damage was done by calculating the area affected based on pixel-wise segmentation metrics. In the proposed method, high segmentation accuracy reduces the false positives and improves the identification of pests. Performance evaluation using accuracy, precision, recall and f-measure shows model reliability. In these findings the proposed segmentation method achieves 99.53 accuracy values compared to other existing methods. Future enhancements include real-time deployment with IoT-based monitoring systems and hyperspectral imaging for further improving the accuracy of detection. It will contribute to precision agriculture, helping farmers in early pest detection and efficient pest management strategies.

Keywords: Adaptive median neural network, Denoising, Maize crop, Pests, Segmentation.

I INTRODUCTION

One of the major staple crops in the world, maize as a food crop has helped in securing food and economic stability to millions of people [1-4]. Infestation by pests severely threatens the productivity of maize by damaging leaves and, in turn, reducing yield. Here, Armyworms [5], [6] Aphids [7], [8], Grasshoppers [9], and Beetles [10] are common pests and among the most destructive ones. The detection and quantification of pest-inflicted damage on plant leaves are crucial for pest management and precision agriculture. Traditional pest monitoring depends on time-consuming manual inspection, human error, and scalability issues among larger agricultural expanse [11-14]. Incorporating the novel techniques of artificial intelligence (AI), especially using deep learning-based computer vision methods, would automate the process of making an assessment of pest damage highly accurately and efficiently [15-17].

Pest detection on maize leaves is rendered difficult by several factors, such as background environmental conditions, intricate leaf structure, and noise in the acquired images. Conventional image processing techniques such as thresholding and edge detection seldom provide a firm segmentation of the affected areas, as variable lighting, occlusions, and noise may prevent accurate analysis. Currently available deep learning methods are also poor at recognizing different damage patterns due to different pest species [18], [19]. Noise introduces an entirely new obstacle to segmentation accuracy, causing false positive regions and other problems within an

otherwise possible pest classification of the affected area [20]. In this regard, robust approaches are needed to diminish noise while preserving critical feature information of the image, followed by state-of-the-art segmentation methods to accurately classify and quantify leaf damage from different pests [21-26].

Upon identifying these challenges, here formulated a two-stage approach which employs deep learning techniques to detect and quantify maize leaf damage:

In the first step, AMNN is applied to combine an advance median filter that adapts the window size according to local features, for the purpose of noise removal from maize leaf images. After noise removal, these images are continuously fed as an input for the segmentation process.

After denoising, the Enhanced Mask R-CNN model performs the segmentation of damaged leaf areas. The model is composed of a Region Proposal Network (RPN) that detects affected areas and a mask prediction branch that generates pixel-wise segmentation masks. With delineation of object boundaries and restriction of false positives, this formulation leads to accurate identification and quantification of pest-induced leaf damage. The percentage of leaf damage is calculated as the ratio of the number of affected pixels to the total leaf area after the segmentation. The model is trained to classify damage caused by different pests; the results showed that Armyworms cause the highest percentage of damage, followed by Aphids, Grasshoppers, and Beetles.

Objective of the paper: Aims of this study are to create an automated system for detecting and quantifying maize leaf damage through a two-step process namely (i) remove noise in leaf image using Adaptive Median Neural Network (AMNN) and (ii) segmentation procedure with Enhanced Mask Region Based-Convolutional Neural Network (Mask R-CNN). To increase the accuracy of delineating infected zones and calculate percentage damage in this case, from these different pests.

Contribution: This Research has competent precision agriculture, in delivering an automated and prospective evaluation of maize leaves for pest damage. By optimizing AMNN for image denoising after that the proposed method leads to further segmentation accuracy using Enhanced Mask R-CNN. The outcomes offer measures on the level of damage due to pest that helps farmer’s specific approach towards pesticide intervention.

ISSN: 1311-1728 (printed version); ISSN: 1314-8060 (on-line version)

Organization: The remaining sections of the paper are organized as follows: Section 2 review related studies on image denoising and segmentation applications for Crop field. Section 3 is to present the proposed approach mainly laid out on AMNN-based denoising and Mask R-CNN-based Segmentation. Experimental results and evaluation metrics are discussed in section 4, finally in section 5; here conclude the paper and point out potential future works.

II RELATED WORKS

Chisonga et al. [27] examine the effects of fall armyworm (Spodoptera frugiperda), an American invasive pest, on maize yield. The insect has since its entry in Africa posed a significant food security threat, particularly in nations that rely on maize as a primary

crop. The study demonstrates how varying degrees of defoliation of leaves by larvae influence maize growth and productivity. Understanding of this relationship is central to the formulation of effective pest control and minimizing yield loss. The study is useful to farmers and policymakers who want to enhance the resilience of maize production.

Toepfer et al. [28] contrasted to harmonize and streamline leaf damage rating scales for assessing fall armyworm (Spodoptera frugiperda) damage in maize. The authors sought to develop a streamlined and harmonized system for application in the field for easier use, thus optimizing pest management and control practices. The streamlining rating system offers an easy way of applying the infestation severity rating by farmers and researchers to enable rapid decision-making in pest control operations.

Baudron et al. [29] researched the major determinants of fall armyworm damage to Eastern Zimbabwean smallholder maize production. It establishes the extent to which planting time, management of the field, and climate shape the level of pest infestation intensity. The research further estimates the economic and yield losses associated with armyworm damage, shedding light in an informative way on the effect of the pest on maize productivity and food security in the region.

Chudik et al. [33] researches present a grasshopper mobile, real-time pest detection system based on image processing and data aggregation technology. The system allows early identification of pests that infest crops, enabling efficient monitoring and control. The system can be deployed in the field, and real-time data collection and analysis will enable farmers to react in time against infestations, hence preventing crop loss and improving pest management.

2.1 Problem Identification

Maize crop is extremely prone to infestations by several pests, for example, armyworms, aphids, grasshoppers, and beetles. Despite many research papers attempting to make conclusions about the prevalence of an individual pest, there is highly limited work conducted on determining relative damage by a combination of pests on the leaf component of maize. Much of the existing literature does not state the degree of damage in percent, which renders their applications toward effective overall insect control less beneficial. This inability to quantify multi-pest damage presents an issue with optimal control measure prioritization. A detection system must then be established that detects the presence of many pests

International Journal of Applied Mathematics
Volume 38 No. 11s, 2025
ISSN: 1311-1728 (printed version); ISSN: 1314-8060 (on-line version)

simultaneously and quantifies leaf damage so that it may aid in maximizing pest management as well as the protection of maize yield.

III MATERIALS AND METHODS

In this paper, aim to detect the percentage of maize leaf damage. Here used four semi supervised datasets from Roboflow and Mendeley to assess the affected areas. This study focuses on maize leaf damage caused by Armyworm, Aphids, Grasshoppers, and Beetles. In the first step, denoise the images using an Adaptive Median Neural Network (AMNN). Then, here apply Enhanced Mask Region-Based Convolutional Neural Network (Mask R-CNN) for segmentation to accurately identify and quantify the affected regions.

Figure 1 shows the maize leaf damage detection process using Enhanced Mask R-CNN. Firstly, image pre-processing includes the re-sizing, normalization, and tensor conversion of the maize leaf. Then, the AMNN is utilized to filter out the noise while keeping the details in the image. Finally, the Enhanced Mask R-CNN model is used for feature extraction and proposal region generation, and the pest-affected region in an input image is segmented.

Post-processing and refinement are done to enhance the accuracy by filtering false positives. The pest classification module identifies the responsible pest type. To conclude, evaluation and accuracy assessment are performed by means of IoU and Dice Coefficient metrics for obtaining the precise segmentation results.

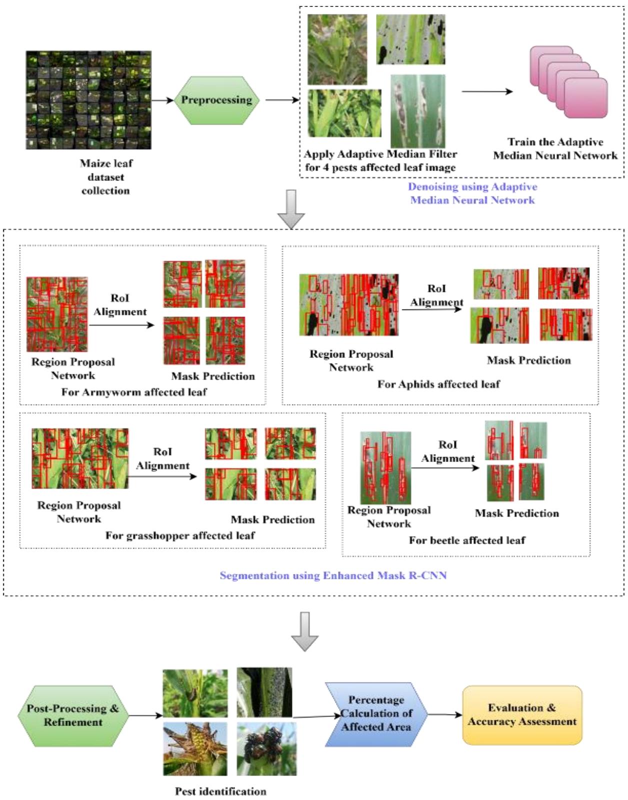

Figure 1: Overall workflow of detect the percentage of Maize Leaf Damage.

3.1 Dataset collection

This paper taken semi supervised dataset from roboflow and mendeley datasets for affected percentage in maize leaf by Armyworm, Aphids, Grasshopper, and Beetle pests.

Dataset1: https://universe.roboflow.com/cdac-evger/maizefall-army

Armyworm Dataset contains 2000 images at 640x640 resolution, and combined they total 103 MB. These are three classes as such: Fall Armyworm Egg (first infestation), Fall Armyworm Frass indicates the location of larvae with waste deposits and Fall Armyworm Larva (the stage of caterpillar's feed maize leaves). The dataset plays a vital role in machine learning models for the early detection and management of fall armyworm infestations in maize fields with less loses.

Dataset2: https://universe.roboflow.com/search?q=class:aphid

The Aphids data has 2000 images of size 210x239 pixels and is around 226 MB in total dataset. Aphids have three classes: Egg — the first aphid stage in development; Nymph (immature feeding, growth stage) which differentiates from adults able reproduce very fast. This dataset is the base for machine learning models that are learning to detect/monitor aphid infestation and consequently, its application will facilitate the pest management in agricultural crops.

Dataset3: https://data.mendeley.com/datasets/bwh3zbpkpv/1

Grasshopper dataset has 2000 images (400×400 pixels) and 91.1 MB, contains 4 classes — Egg (the first stage of development); Nymph (grasshopper juvenile stage when they begin to ingest the vegetation) and Adult that is capable of destroying large amount of crops.

The dataset is good for training the machine learning models that can classify and detect the grasshoppers for insect control as well to get better yield from your farmland.

Dataset4: https://data.mendeley.com/datasets/bwh3zbpkpv/1

Beetle dataset consists 2000 images each having a resolution of 400*400 In total, the dataset is 63.5 MB. Classes are Egg (stage of first development), Larva – also known as active feeding stage that will destroy crops; Pupa which comes before adulthood; and the Adult an adult stage that can reproduce and fee listening. This will be a very useful dataset for training machine learning models that are going to be detecting beetles and classifying them for (insect) pest management, etc.

3.2 Denoising using Adaptive Median Neural Network

Adaptive Median Neural Network (AMNN) is a hybrid denoising model which cooperates with adaptive median for filtering and optimizes the neural network to denoise an image but also retains essential features such as edges and textures. In this step, AMF is used as a preprocessor to detect and reduce noise—mainly impulse noise (salt-and-pepper noise)—by dynamically adjusting the filter size according to local pixel variations. However, median filtering alone may cause image blurring, leading to loss of fine details.

This is overcome by passing the output from AMF through a Neural Network, often a Convolutional Neural Network (CNN) or Autoencoder, which learns to reconstruct the clean image from the filtered input. The NN refines the denoised image by restoring lost details, improving the overall quality of the image. The AMNN is trained on a noisy and ground truth image dataset by optimization of loss functions like Mean Squared Error (MSE) or Structural Similarity Index (SSIM). Such a hybrid approach is especially useful in applications of medical imaging, remote sensing, and low-light photography, where preserving fine image details matters much.

3.2.1 AMNN used in denoising the affected maize leaf

The AMNN denoising method improves the pest infested maize leaf detection by first denoising the images through Adaptive Median Filtering (AMF) and then fine-tuning it using a Neural Network by Shrestha [40]. Image segmentation techniques are used to select the damaged areas by the attack of Armyworm, Aphids, Grasshopper, and Beetle after denoising. The percentage of the affected maize leaf is estimated by finding the ratio of damaged to total leaf area pixels. This method provides precise pest damage analysis and maintains the basic structure information of leaves.

The Adaptive Median Filter (AMF) dynamically adjusts its window size based on local pixel intensity variations to remove salt-and-pepper noise while preserving edges.

$I_{filtered}(x, y) = median\ \{I(i, j) | (i, j) \in S(x, y)\}$ ------ (1)

Where, $I(i, j)$ is the pixel intensity in the original noisy image. $S(x, y)$ is the adaptive neighborhood window centered at (x, y). $I_{filtered}(x, y)$ is the output of the median filter for the pixel at (x, y). In equation (1) the window size $S(x, y)$ is increased until a non-noisy median value is found, ensuring effective noise removal. This formula helps remove salt-and-pepper noise and preserve leaf damage patterns by computing the median value of pixel intensities within an adaptive neighborhood window $S(x, y)$.

In equation (2) the NN refines the AMF output to reconstruct a clean image by learning a mapping function from noisy to clean images.

$I_{denoised} = f_\theta(I_{filtered})$ ---------- (2)

Where, $I_{filtered}$ is the AMF-processed image. f_θ represents the AMNN model with learnable parameters θ. $I_{denoised}$ is the final denoised image used for leaf damage detection.. This equation (2) represents how the AMNN model processes the filtered image to refine it further and reconstruct a cleaner image.

Use image thresholding or deep learning segmentation to detect pest-damaged areas. Convert the denoised image to a binary mask.

$M(x, y) = \begin{cases} 1, & I_{denoised}(x, y) < T \\ 0, & I_{denoised}(x, y) \geq T \end{cases}$ - ----- (3)

Where, $M(x, y)$ is binary mask (1 for affected, 0 for healthy). T is threshold for identifying affected pixels.

Calculate the percentage of damaged leaf area relative to the total leaf area.

ISSN: 1311-1728 (printed version); ISSN: 1314-8060 (on-line version)

$Affected\ percentage = \left(\frac{\sum \mathrm{M(x,y)}}{\sum \mathrm{P(x,y)}}\right) \times 100$ ---- (4)

$\mathrm{M(x,y)}$ is total number of affected pixels. $\sum \mathrm{P(x,y)}$ is total number of pixels in the leaf area.

The neural network is trained by minimizing a loss function:

$L = \frac{1}{N}\sum_{i=1}^{N}(I_{clean}(i) - I_{denoised}(i))^2$ --- (5)

Where, $I_{clean}(i)$ is the ground truth clean image pixel. $I_{denoised}(i)$ is the output from AMNN. N is the total number of pixels. Equation (5) is the Mean Squared Error (MSE) loss function, which measures the difference between the clean ground truth image and the denoised image output from AMNN. Minimizing this loss during training ensures the AMNN model learns to generate accurate clean images.

Once the image is denoised using AMNN, its quality is evaluated using three key metrics**:**

Peak Signal-to-Noise Ratio (PSNR):

$PSNR = 10\ log_{10}(\frac{(L_{max})^2}{MSE})$ -------- (6)

Where, L_{max} is the maximum possible pixel value. Higher PSNR indicates better denoising quality of leaf image. Equation (6) PSNR quantifies the quality of the denoised image by measuring how much the denoised image deviates from the clean image.

Structural Similarity Index (SSIM):

$SSIM = \frac{(2\mu_x\mu_y + C_1)(\sigma_{xy} + C_2)}{(\mu_x^2 + \mu_y^2 + C_1)(\sigma_x^2 + \sigma_y^2 + C_2)}$ ---------- (7)

Equation (7) measures structural similarity between the clean and denoised images. SSIM compares the structural information (contrast, luminance, and texture) between the clean and denoised damaged leaf images. Unlike PSNR, which only considers pixel differences, SSIM evaluates how well the structure and details are preserved. A value close to 1 indicates high similarity, meaning better denoising performance.

Root Mean Squared Error (RMSE):

$RMSE = \sqrt{MSE}$ ----------- (8)

In equation (8) lower RMSE values indicate better denoising performance. RMSE measures the overall pixel-wise error between the denoised and ground truth leaf images. A lower RMSE value indicates a better denoised image with fewer distortions.

ISSN: 1311-1728 (printed version); ISSN: 1314-8060 (on-line version)

Figure 2 shows the AMNN denoising process of maize leaf images infested with pests such as

Algorithm 1: Adaptive Median Neural Network using in Denoising

Inputs:
Noisy Image I_{noisy}
Ground Truth Image I_{clean} (for training phase)
AMNN Model f_θ
Training Parameters: Learning Rate η, Number of Epochs E
Step 1: Apply AMF (I_{noisy}):
 Initialize output image $I_{filtered}$
 For each pixel (x, y) in I_{noisy}:
  Define adaptive window S(x, y)
  Compute median value of pixels in S(x, y)
  If median value is a non-noisy pixel:
   Set $I_{filtered}(x, y)$ = median value
  Else:
   Expand window S(x, y) and repeat
 End For
 Return $I_{filtered}$
Step 2: Train (AMNN) (I_{noisy}, I_{clean}, AMNN model, learning rate (η), epochs E):
 Initialize model parameters θ
 For epoch = 1 to E:
  For each training pair (I_{noisy}[i], I_{clean}[i]):
   $I_{filtered}$= Apply AMF (I_{noisy}[i])
   $I_{denoised}$ = AMNN model ($I_{filtered}$)
   Compute loss:
    $L = \frac{1}{N}\sum_{i=1}^{N}(I_{clean}(i) - I_{denoised}(i))^2$
   Update model parameters θ using gradient descent:
    θ = θ - η * ∇L (θ)
  End For
 End For
 Return Trained AMNN model
Step 3: Denoise with AMNN (I_{noise}, Trained AMNN model):
 $I_{filtered}$= Apply AMF (I_{noise})
 $I_{denoised}$ = Trained AMNN model ($I_{filtered}$) Return $I_{denoised}$
Step 4: Evaluate Denoised Image (I_{clean}, $I_{denoised}$):
 Compute PSNR:
  $PSNR = 10\ log_{10}(\frac{(I_{max})^2}{MSE}$
 Compute SSIM:
  $SSIM = \frac{(2\mu_x\mu_y+C_1)(\sigma_{xy}+C_2)}{(\mu_x^2+\mu_y^2+C_1)(\sigma_x^2+\sigma_y^2+C_2)}$
 Compute RMSE:
  $RMSE = \sqrt{MSE}$
 Return PSNR, SSIM, RMSE
Output:
Denoised Image $I_{denoised}$

Armyworm, Aphids, Grasshoppers, and Beetles. First, it starts with preprocessing, whereby noisy images are resized, normalized, and filtered to improve their quality. The preprocessed image is then passed through the AMNN model, which applies adaptive median filtering followed by neural network-based noise removal while preserving important leaf details.

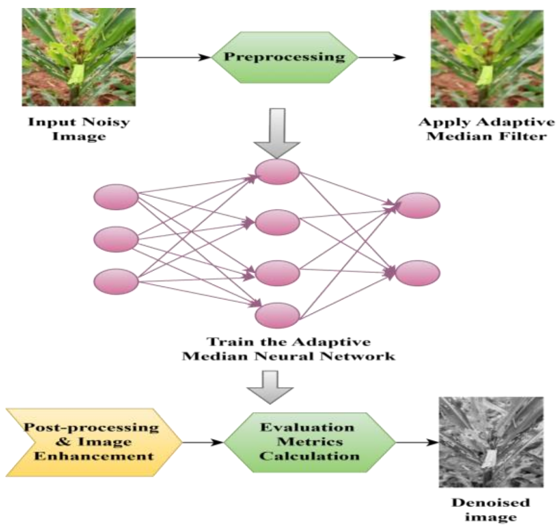

Figure 2: Denoising using AMNN

Volume 38 No. 11s, 2025
ISSN: 1311-1728 (printed version); ISSN: 1314-8060 (on-line version)

This then provides the denoised output with a clearer version for further analysis. In the last stage of the quality evaluation metrics calculation, the denoising quality is evaluated using PSNR, SSIM, and RMSE for ensuring that the noise reduction is done correctly.

Algorithm 1 and Figure 3 the Adaptive Median Neural Network (AMNN) denoising algorithm improves the quality of noisy images through a combination of Adaptive Median Filtering (AMF) and deep learning-based refinement. It first utilizes AMF to eliminate salt-and-pepper noise but keeps the basic characteristics of the original image. The image filtered by AMF is passed into the AMNN model, where it learns how to reconstruct the cleaner image through a mapping function trained on pairs of noisy images and their corresponding ground truths.

The model parameters are optimized during training in order to minimize the loss function, which in this case is the Mean Squared Error—MSE—using gradient descent. After training, the AMNN model is ready to be used for the denoising of new images. The performance of the denoised output is evaluated in terms of PSNR (Peak Signal-to-Noise Ratio), SSIM (Structural Similarity Index), and RMSE (Root Mean Squared Error) to validate the accurate noise removal while keeping the image details.

Figure 3: Adaptive Median Neural Network Flow diagram

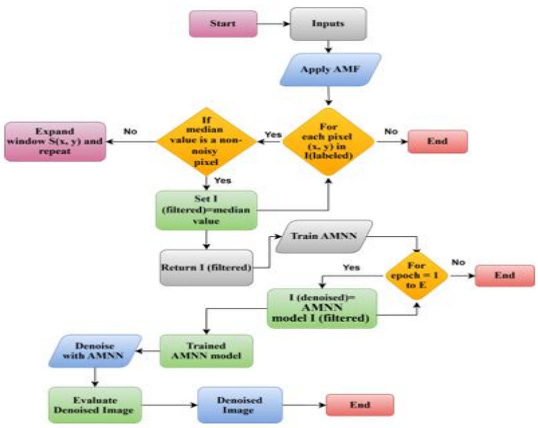

3.3 Segmentation using Enhanced Mask Region-Based Convolutional Neural Network

3.3.1 RCNN

Region-Based Convolutional Neural Network (RCNN) is a deep learning-based object detection technique that detects objects in images by first proposing regions and then classifying them with a Convolutional Neural Network (CNN). Research by Li, et al. [41] eases the task of object detection, segmentation, and localization by extracting meaningful features from each proposed region. In the detection of maize leaf-affected percentages, RCNN first extracts regions of interest (RoIs) from an image through a selective search. The regions are then passed through a CNN for classification of the pest damage caused by Armyworm, Aphids, Grasshopper, or Beetle attacks; a segmentation process aids in measuring the affected area of the maize leaves. It thereafter calculates the percentage of damage by comparing the segmented area affected with the total leaf area.

Volume 38 No. 11s, 2025
ISSN: 1311-1728 (printed version); ISSN: 1314-8060 (on-line version)

The limitations of RCNN include high computational cost because the process for every region proposal is done individually; hence, it's slow and less efficient in real-time applications. It also comprises large storage in handling extracted features and is not end-to-end trainable since it has many independent steps, which are region selection, feature extraction, and classification, thus making it hard to optimize. In addition, RCNN is not good at precise segmentation for fine details, resulting in lower precision in the detection of maize leaf damage percentages. The drawbacks of those mentioned above necessitate to resort to Enhanced Mask R-CNN which speeds up detection & estimate and quality, also segmentation.

In order to overcome the aforementioned shortcomings, Enhanced Mask R-CNN provides object detection and segmentation with faster, accurate predictions.

In comparison to RCNN, RPN in Enhanced Mask R-CNN executes the whole image, where it is trying to mitigate wasteful computation. The enhanced variant further boosts the accuracy of segmentation by the methods such as attention mechanisms and features fusion which facilitate with precise detection of leaf area affected by pest on maize-crop in real time.

3.3.2 Enhanced Mask RCNN

R-CNN (Region-Based Convolutional Neural Networks — Improved Mask) — an advanced segmentation technique combined with deep learning method used for detecting objects and pixel wise classification are implemented here. Exploiting the Mask R-CNN architecture, this work focuses on improvement in attention feature fusion with improved region proposal networks for better accuracy. It consists of: 1) detecting regions of interest with RPN, 2) classifying objects and finally (3) obtain segmentation mask for each instance. After thorough object boundary refining and extraction, Enhanced Mask R-CNN is strong enough to work on tasks, even the challenging ones like those with diseased or pest-affected areas present in agricultural images.

The Enhanced Mask R-CNN improves the segmentation of pest-infested maize leaf areas by accurate detection and outlining of damage caused by Armyworm, Aphids, Grasshopper, and Beetle attacks. It uses a Region Proposal Network (RPN) for the identification of affected regions and a mask prediction branch for pixel-wise segmentation. The approach refines object boundaries and reduces false positives, hence ensuring the exact computation of the affected maize leaf percentage, helping in effective pest damage assessment.

$$M(x,y) = \begin{cases} 1, if\ pixel\ (x,y) is\ classified\ as\ affected \\ 0, otherwise \end{cases} \text{----------- (9)}$$

Where $M(x,y)$ represents the binary mask generated by Enhanced Mask R-CNN. **1**: Pixel is affected by a pest. **0**: Pixel is healthy. Equation (9) represents the binary segmentation mask, where affected regions are marked as 1, and unaffected areas are marked as 0.

$$A_d = \sum_{x=1}^{W} \sum_{y=1}^{H} M(x,y) \text{ ------------- (10)}$$

Where $A_d$the total number of affected pixels, W and H is are the image width and height. Equation (10) calculates the total number of affected pixels by summing up all 1's in the binary mask.

ISSN: 1311-1728 (printed version); ISSN: 1314-8060 (on-line version)

$A_l = \sum_{x=1}^{W} \sum_{y=1}^{H} L(x, y)$ ------------- (11)

Where $A_l$the total number of pixels corresponding to the maize is leaf, and $L(x, y)$represents the binary leaf mask. Equation (11) determines the total number of pixels corresponding to the maize leaf.

$P_a = \frac{A_d}{A_l} \times 100$ --------- (12)

Where P_a gives the percentage of the maize leaf affected by pests. Equation (12) computes the percentage of the maize leaf affected by pests, which is crucial for assessing damage severity.

Intersection over Union (IoU) for Accuracy Evaluation:

$IoU = \frac{M_p \cap M_{GT}}{M_p \cup M_{GT}}$ ------------- (13)

Where M_p is the predicted mask, and M_{GT} is the ground truth masks. Equation (13) represents IoU measures the accuracy of segmentation by evaluating the overlap between the predicted and actual affected regions. A higher IoU value indicates better segmentation performance.

$D = \frac{2 \times M_p \cap M_{GT}}{|M_p| + |M_{GT}|}$ --------- (14)

Equation (14) Measures the overlap between the predicted and actual affected regions. The Dice coefficient quantifies the similarity between the predicted and actual segmentation masks. A higher Dice score indicates better segmentation accuracy. The workflow of the Enhanced

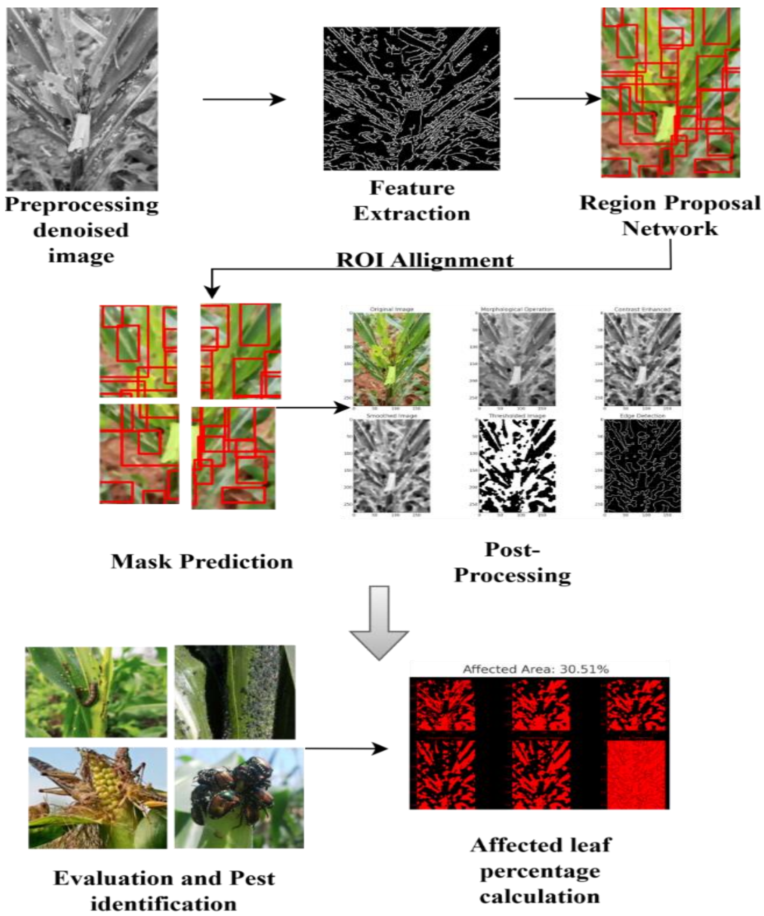

International Journal of Applied Mathematics
Volume 38 No. 11s, 2025
ISSN: 1311-1728 (printed version); ISSN: 1314-8060 (on-line version)

Mask R-CNN in Figure 4 first begins with the preprocessing stage, where an input image is resized to a specified size, normalized, and converted into a tensor format. Then, features involved in pest damage patterns and textures are extracted by the backbone CNN. The Region

Figure 4: Segmentation using Enhanced Mask R-CNN

Proposal Network (RPN) then generates candidate object regions by filtering out unimportant background regions.

Through RoI alignment, these regions are resized and aligned for accurate segmentation. The mask prediction step generates pixel-wise segmentation masks to outline the pest-affected areas precisely. In post-processing, the masks are refined, false positives are reduced as much as possible, and the affected areas are quantified.

Next comes the evaluation and classification of pests, in which segmentation accuracy is evaluated with IoU and Dice Coefficient, and a classifier identifies the type of pest, such as Armyworm, Aphids, Grasshopper, and Beetle. Finally, percentage calculation is performed to obtain the ratio of affected leaf area by calculating the ratio of damaged to the total leaf pixels, thereby enabling a precise assessment of pest impact.

Enhanced Mask R-CNN segmenting is done, then it is found that Armyworm causes the highest percentage of damage to maize leaves, followed by Aphids, Grasshoppers, and Beetles.

Algorithm 2 and Figure 5 present the enhanced mask R-CNN algorithm used for segmenting and analyzing maize leaf damage caused by pests such as armyworm, aphids, grasshoppers, and beetles. The following steps first pre-process the input image by resizing, normalizing, and converting it into a tensor. Then, the model is trained with a combination of Binary Cross-Entropy and Dice Loss to improve the accuracy of segmentation. Once trained, the model segments the damaged leaf regions, calculates the percentage of affected area, and classifies

Algorithm 2: Segmentation using Enhanced Mask R-CNN

Inputs: $I_{input} \rightarrow$ Input maize leaf denoised image, Pre-trained Mask R-CNN model M_θ, Threshold values for segmentation and classification
Training Parameters: Learning Rate (η), Number of Epochs (E)
Begin:
Step 1: Preprocess Image (I_{input}):
  Resize I_{input} to fixed dimensions (e.g., 1024x1024)
  Normalize pixel values (0 to 1)
  Convert to tensor format
  Return preprocessed image ($I_{preprocessed}$)
Step 2: Train Enhanced Mask RCNN (Dataset, Model M_θ, Learning Rate η, Epochs E):
  Initialize model parameters θ
  For epoch = 1 to E:
    For each training image I_{input} and ground truth mask M_{GT}:
      $I_{preprocessed}$ = Preprocess Image (I_{input})
      Predicted mask M_p = Model M_θ ($I_{preprocessed}$)
      Compute Loss L:
        L = Binary Cross-Entropy (M_p, M_{GT}) + Dice Loss (M_p, M_{GT})
      Update Model Parameters:
        θ = θ - η * ∇L (θ)
    End For
  End For
  Return Trained Model M_θ
Step 3: Segment Leaf Damage (I_{input}, Trained Model M_θ):
  $I_{preprocessed}$ = Preprocess Image (I_{input})
  $M_p = M_\theta$ ($I_{preprocessed}$)
  Affected Area = Count Non-Zero Pixels in M_p
  Total Leaf Area = Count Non-Zero Pixels in Leaf Mask
  $P_a = \frac{A_d}{A_l} \times 100$
  Return M_p, P_a
Step 4: Classify Pest (M_p, Trained Model M_θ):
  Extract features from affected regions
  Apply trained pest classifier
  Pest Label = Argmax (Model M_θ (M_p))
  Return Pest Label
Outputs:
Segmentation mask of affected regions
Percentage of affected leaf area
Pest classification (Armyworm, Aphids, Grasshopper, Beetle) (Ctrl)

International Journal of Applied Mathematics
Volume 38 No. 11s, 2025
ISSN: 1311-1728 (printed version); ISSN: 1314-8060 (on-line version)

the pest responsible for the damage. The percentage of affected area (P_a) is calculated by comparing the damaged region to the total leaf area. The final output will be a segmentation mask, the extent of damage, and the identified pest type, which helps in early pest detection and precision agriculture strategies

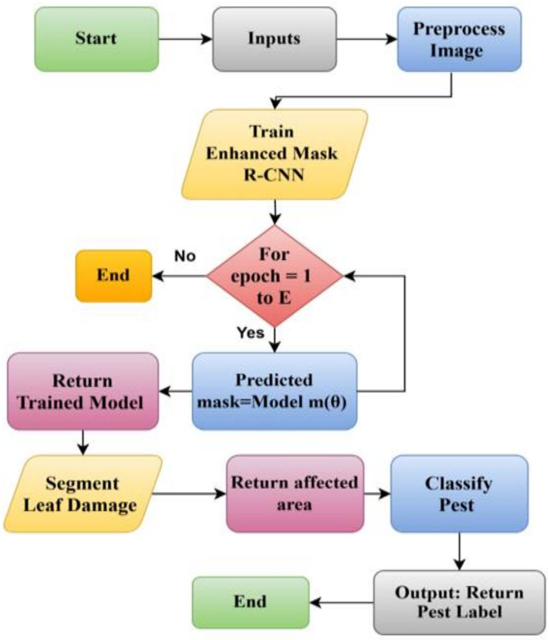

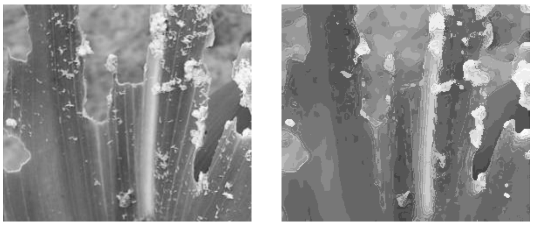

Figure 6: Denoising Results (Fall Armyworm)

Figure 5: Enhanced Mask R-CNN Flow Diagram

IV RESULTS AND DISCUSSIONS

This paper developed by Python to detect maize leaf damage percentage caused by Armyworm, Aphids, Grasshoppers, and Beetles. Results show that the Enhanced Mask R-CNN model can effectively achieve the segmentation and quantification of pest-induced damage on maize leaves. After denoising with the Adaptive Median Neural Network (AMNN), the segmentation of affected regions became clearer. Here taken 4 datasets from roboflow and mendeley pest datasets for calculating the affected maize lead percentage. Among the detected pests, Armyworm, Aphids, Grasshoppers, and Beetles the Armyworm damaged highest percentage of maize leaf damage. Evaluation metrics confirmed segmentation accuracy, showing high accuracy and hence ensured reliable pest damage assessment. The proposed Enhanced Mask

R-CNN achieves the 99.53% accuracy in detecting the pest affected leaf percentage calculation.

A percentage of the affected leaf area for each pest type was also calculated for precise pest impact evaluation. The results demonstrate the potential of this approach in the early detection of pests and for precision agriculture in order to provide farmers with timely preventive measures.

4.1 Denoising and Segmentation Results

4.1.1 Fall Armyworm

Figure 6 reveals the efficiency of the Adaptive Median Neural Network (AMNN) denoising. The noisy original image (left) has extreme visual interruptions and is difficult to analyze. The image is brighter after denoising (right), with visible details such as texture of leaves and detectability of pests for simpler detection and analysis

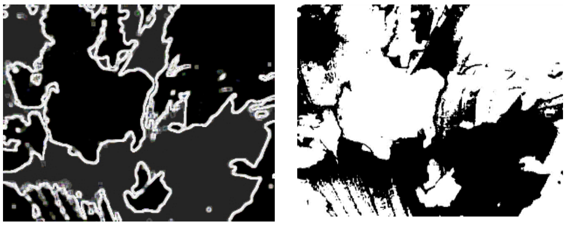

Figure 7: Segmentation Result (Fall Armyworm)

Figure 7 depicts the outcome of segmentation, in which the original image includes an infestation of a pest on a maize leaf. Following segmentation, the background is eliminated, leaving only the pest and damaged leaf area isolated. This provides improved focus on the area of interest, facilitating easier subsequent analysis, such as pest detection or damage measurement.

4.1.2 Aphids

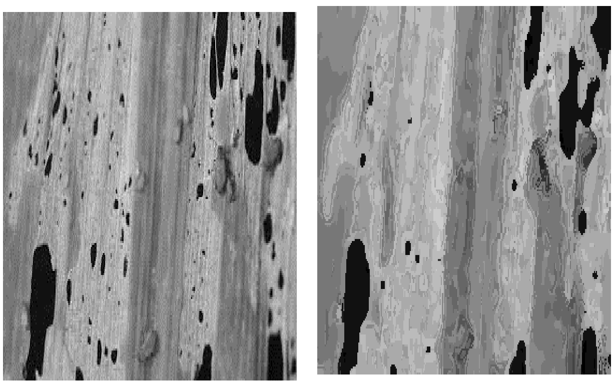

Figure 8: Denoising Result (Aphids)

International Journal of Applied Mathematics
Volume 38 No. 11s, 2025
ISSN: 1311-1728 (printed version); ISSN: 1314-8060 (on-line version)

Figure 8 illustrates the denoising outcome of an aphid-infected plant surface. The noisy input image on the left-side of the figure contains visual noise which hides minute details. The denoised output via AMNN on the right side properly eliminates noise, improving clarity and the separability of aphid infected regions and surface textures.

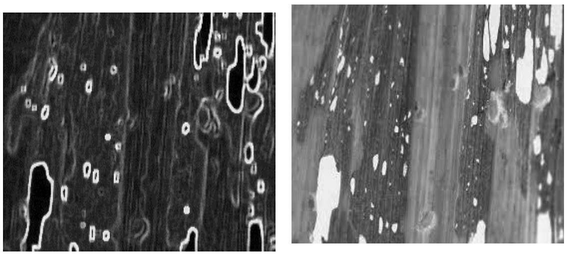

Figure 9: Segmentation Result (Aphids)

Figure 9 contrasts a healthy leaf with an aphid-infected leaf and its segmented counterpart. In the segmented image, the background and unnecessary space are eliminated such that only damaged leaf space and aphid-damaged space remain. Segmentation provides more emphasis on priority regions, enabling better analysis of damage severity and aphid infection.

4.1.3 Grasshopper

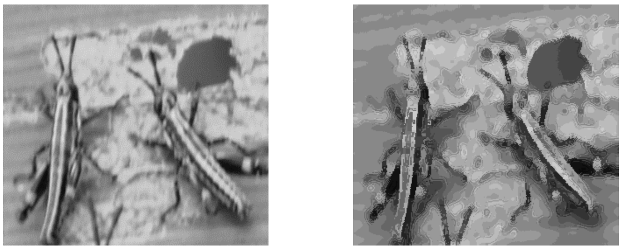

Figure 10: Denoising Result (Grasshopper)

Figure 10 contrasts a noisy input image and denoised image using AMNN for an infested plant with grasshoppers. The left noisy image has visual interferences that hide fine details. Upon denoising, the right image is clearer, with less noise and sharper textures, such that the plant structure and grasshopper infestation are more discernible.

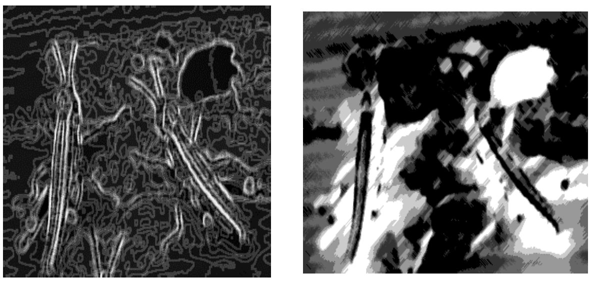

Figure 11: Segmentation Result (Grasshopper)

Figure 11 shows the original input and the segmented output for an infested grasshopper plant. From the original image, one can observe that there is damage to the plant caused by grasshoppers on the leaves. The segmented image distinctly delineates the damaged areas so

ISSN: 1311-1728 (printed version); ISSN: 1314-8060 (on-line version)

that the damaged areas visible background is rejected, allowing for easy focus on pest-related damage for analysis.

4.1.4 Beetle

Figure 12: Denoising Result (Beetle)

Figure 12 shows the denoising result of Beetle-infected plants. The noisy input, shown on the left, shows lower visual clarity due to noise interference. The image on the right, denoised by applying the AMNN denoising technique, minimizes noise to a great extent, making the plant structures and regions of beetle infection more distinct for further analysis.

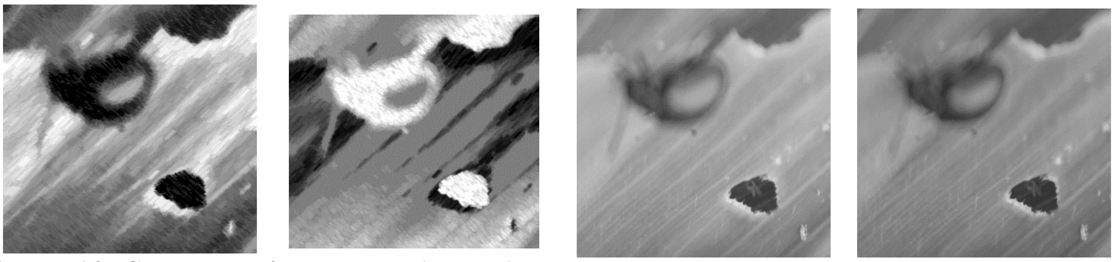

Figure 13: Segmentation Result (Beetle)

Figure 13 is the segmentation result of Beetle-damaged leaves. The left image is the original input, with visible damage from beetles. The right image is the segmented output, successfully separating the damaged

area from the rest of the healthy leaf to better detect and analyze pest damage.

4.2 Performance metrics

4.2.1 Accuracy

In predictive modeling, accuracy is the measure of closest model's projections is to real-world outcomes. It evaluates the model because many choices and forecasts rely on its accuracy and dependability.

T-True, F-False, P-Positive, N-Negative

$Accuracy = \frac{TP+TN}{TP+TN+FP+FN}$ ------- (15)

4.2.2 Precision

In predictive modeling, accuracy is the proportion of total expected positive observations to correctly forecast positive observations it demonstrates the model's successful reduction of false positives, guaranteeing that the positive forecasts it delivered are accurate and reliable by extension and error reduction in many other domains.

$Precision = \frac{TP}{TP+FP}$ ------ (16)

4.2.3 Recall

Volume 38 No. 11s, 2025
ISSN: 1311-1728 (printed version); ISSN: 1314-8060 (on-line version)

Recall in predictive modeling is the fraction of real positive instances properly detected in the model. In sectors like disease detection, identifying all positives is critical since it shows the efficient detection of all relevant instances in a particular class.

$Recall = \frac{TP}{TP+FN}$ ------ (17)

4.2.4 F-measure

F-measure, which determines the harmonic mean of recall and accuracy, is a strong all-around measurement of the efficient performance in model that is necessary for preventing both false positives and false negatives.

$F - measure = 2 \times \frac{Precision \times recall}{precision+recall}$ ------- (18)

Table 1: Comparison table for Denoising

	Algorithms/ Metrics	**PSNR**	**SSIM**	**RMSE**
Dataset 1	**NLM [42]**	12.76	0.52	0.21
	Wavelet [43]	13.34	0.58	0.20
	AMF [44]	13.76	0.62	0.19
	AMNN (Proposed)	14.71	0.66	0.18
Dataset 2	**NLM [42]**	12.66	0.49	0.24
	Wavelet [43]	13.14	0.51	0.21
	AMF [44]	13.46	0.59	0.19
	AMNN (Proposed)	14.21	0.62	0.15
Dataset 3	**NLM [42]**	12.70	0.40	0.22
	Wavelet [43]	13.25	0.47	0.20
	AMF [44]	13.32	0.52	0.17
	AMNN (Proposed)	14.41	0.58	0.15
Dataset 4	**NLM [42]**	12.18	0.49	0.23
	Wavelet [43]	12.94	0.52	0.21
	AMF [44]	13.31	0.60	0.18

Received: August 06, 2025

ISSN: 1311-1728 (printed version); ISSN: 1314-8060 (on-line version)

	AMNN (Proposed)	13.99	0.62	0.14

Table 1 compares the four algorithms such as NLM, Wavelet, AMF, and proposed AMNN over four different datasets using three evaluation metrics: PSNR, SSIM, and RMSE. PSNR values for the proposed AMNN algorithm were consistently higher, signifying better image quality restoration. In a similar thread, the values of SSIM, defined as structural similarity, also confirm that AMNN is superior to other methods indicating some improvements in perceived similarity to the ground truth images. The RMSE is markedly less for AMNN in all datasets, showing very little reconstruction error. They also consistently push the performances forward for datasets, further indicating the resilience of AMNN. The results suggest that the proposed method performs better in enhancing image quality compared to traditional approaches. This positions AMNN as the method of choice for image denoising or restoration.

In Dataset 1 compares PSNR, SSIM, and RMSE values across four algorithms: NLM, Wavelet, AMF, and AMNN (Proposed). The AMNN method achieves the highest PSNR and SSIM, indicating better image quality and structural similarity, while also having the lowest RMSE, reflecting minimal error. This confirms the superior performance of the proposed AMNN approach over the other methods. In this chart the x-axis show the denoising algorithms and the y-axis shows the values for metrics.

In Dataset 2 compares PSNR, SSIM, and RMSE values across four algorithms: NLM, Wavelet, AMF, and AMNN (Proposed). The AMNN method achieves the highest PSNR and SSIM, indicating better image quality and structural similarity, while also having the lowest RMSE, reflecting minimal error. This confirms the superior performance of the proposed AMNN approach over the other methods. In this chart the x-axis show the denoising algorithms and the y-axis shows the values for metrics.

In Dataset 3 compares PSNR, SSIM, and RMSE values across four algorithms: NLM, Wavelet, AMF, and AMNN (Proposed). The AMNN method achieves the highest PSNR and SSIM, indicating better image quality and structural similarity, while also having the lowest RMSE, reflecting minimal error. This confirms the superior performance of the proposed AMNN approach over the other methods. In this chart the x-axis show the denoising algorithms and the y-axis shows the values for metrics.

In Dataset 4 compares PSNR, SSIM, and RMSE values across four algorithms: NLM, Wavelet, AMF, and AMNN (Proposed). The AMNN method achieves the highest PSNR and SSIM, indicating better image quality and structural similarity, while also having the lowest RMSE, reflecting minimal error. This confirms the superior performance of the proposed AMNN approach over the other methods. In this chart the x-axis show the denoising algorithms and the y-axis shows the values for metrics.

Received: August 06, 2025

Table 2: Comparison table for Segmentation using 4 different dataset

	Algorithms/ Metrics	Accuracy	Precision	Recall	F-measure
Dataset 1	**YOLO [45]**	98.20	98.01	98.10	97.47
	CNN [46]	98.76	98.27	98.63	98.11
	RCNN [47]	99.13	99.11	99.10	98.36
	Enhanced Mask R-CNN (proposed)	99.53	99.51	99.52	99.50
Dataset 2	**YOLO [45]**	98.03	98.00	98.01	97.90
	CNN [46]	98.41	98.13	98.60	98.11
	RCNN [47]	98.95	98.59	98.91	98.30
	Enhanced Mask R-CNN (proposed)	99.13	98.86	99.02	98.82
Dataset 3	**YOLO [45]**	98.21	97.85	98.09	97.53
	CNN [46]	98.82	98.31	98.42	98.09
	RCNN [47]	99.15	98.96	99.02	98.47
	Enhanced Mask R-CNN (proposed)	99.41	99.07	99.20	99.00
Dataset 4	**YOLO [45]**	98.10	98.00	98.01	97.32
	CNN [46]	98.94	98.63	98.62	98.10
	RCNN [47]	99.21	99.04	99.19	98.82
	Enhanced Mask R-CNN (proposed)	99.50	99.31	99.46	99.19

In table 2 compares the evaluation of the data will target four object detection algorithms, namely YOLO, CNN, RCNN, and the proposed Enhanced Mask R-CNN, on four datasets in terms of Accuracy, Precision, Recall, and F-measure. YOLO shows a consistent but poorer performance in every metric with an accuracy of around 98.03% to 98.21% and an F-measure lying between 97.32% and 97.90%, meaning it is relatively less capable of detecting objects reliably. Compared to YOLO, CNN offers marginal improvements in precision and recall with an accuracy range of 98.41% and 98.94%. RCNN still further improves the performance with an accuracy of up to 99.21% with precision, recall, and F-measure quite

balanced. In all datasets, Enhanced Mask R-CNN gives the best score with an accuracy ranging between

International Journal of Applied Mathematics
Volume 38 No. 11s, 2025
ISSN: 1311-1728 (printed version); ISSN: 1314-8060 (on-line version)

99.13% and 99.53%, thus showing it as the best-performing algorithm. It lends a good balance throughout the metrics, achieving an F-measure of 99.50% in Dataset 1 and almost equally high values in the remaining datasets. This shows that Enhanced Mask R-CNN works much better than YOLO, CNN, and RCNN, and this makes it the best possible option for object detection.

Metrics of Dataset 1,2,3,4 calculate and compare Accuracy, Precision, Recall, and F-measure using different algorithms. The Enhanced Mask R-CNN (proposed) achieves the highest values across all metrics, demonstrating its superior performance. F-measure, indicating slightly lower overall effectiveness.

Table 3: Pests and Leaf Affected Comparison Table

Pest Name	Damage Characteristics	Affected Leaf Percentage	Common Symptoms	Severity
Armyworm	Feeds on leaf tissue, creating large irregular holes and skeletonized leaves	Highest (40-50%)	Ragged edges, complete defoliation in severe cases	Severe
Aphids	Sucks plant sap, causing yellowing and curling of leaves	Moderate (25-30%)	Sticky honeydew, mold growth, stunted plant growth	Moderate
Grasshopper	Chews on leaf margins and midribs, leaving irregular notches	Moderate (20-25%)	Jagged edges, reduced leaf area, sporadic damage	Moderate
Beetle	Feeds on both upper and lower leaf surfaces, causing shot-hole damage	Lowest (10-15%)	Small, round holes, weakening of plant structure	Mild

Table 3 shows the maize leaves affected by Armyworms, Aphids, Grasshopper and Beetle pests. The armyworm is the most serious pest, causing a sheet-like defoliation with an affected leaf area percentage ranging from 40-50%. Moderate damages are caused by aphids and grasshoppers; curling symptoms are there, with honeydew secretion and jagged edges. Least damage is however inflicted by beetles which chew small, round holes on both leaf surfaces, with the area affected 10-15%. Nevertheless, their damage is relatively light

International Journal of Applied Mathematics
Volume 38 No. 11s, 2025
ISSN: 1311-1728 (printed version); ISSN: 1314-8060 (on-line version)

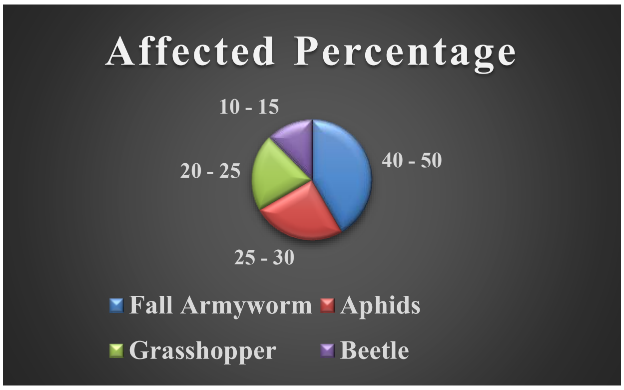

compared to the other pests; whereas, a prolonged infestation renders the structure weak and at risk of being succumbed to other stress factors. The results show the Armyworms are highly affect the maize leaves.

V CONCLUSIONS

This paper proposed a hybrid deep learning approach combining the AMNN for denoising with the Enhanced Mask R-CNN for segmentation for pest-induced damage detection and quantification on maize leaves segmentation. Experimental results proved that our model can locate high-precision areas with great efficacy, suppressing interference from noise hugely. Among the identified pests, which included Armyworm, Aphids, Grasshoppers, and Beetles, the highest percentage of leaf damage was caused by Armyworm. Here taken 4 datasets for finding the results of maize leaf affected percentage. Computed leaf-affected percentage helps in the early detection of pest infestation hence in a timely intervening action for precision agriculture and management of pest control. Though the proposed model gives a high accuracy in segmentation, the Enhanced mask R-CNN achieves 99.53 % accuracy value compared to other existing methods.

Here further suggest, for future enhancements, the integration of a self-learning adaptive system that continuously enhances pest detection based on real-time data collection from IoT-enabled smart farms. This could be further improved by the integration of hyperspectral imaging and thermal imaging techniques, increasing the accuracy of pest detection due to spectral differences in leaf damage. Another improvement would be using attention-based transformer networks for better feature extraction and segmentation. It could be further expanded with more pest species and multi-class classification models to improve generalization across different crop conditions.

Finally, deploying the trained model in a mobile-based or drone-assisted real-time detection system can further help farmers in automating pest surveillance for cost-effective and sustainable pest management strategies. With its continuous updating through more sophisticated deep learning architectures, further improvement is achieved in accuracy regarding pest detection, ensuring further crop yield while minimizing losses owing to pest infestations.

ISSN: 1311-1728 (printed version); ISSN: 1314-8060 (on-line version)

References:

1. Pfordt, A., & Paulus, S. (2025). A review on detection and differentiation of maize diseases and pests by imaging sensors. *Journal of Plant Diseases and Protection*, *132*(1), 1-21.
2. Roy, S., Binu, D., Rajakumar, B. R., Talasila, V., & Bhatt, A. (2024). Super Resolved Maize Plant Leaves Disease Detection Using Optimal Generative Adversarial Network. *International Journal of Image and Graphics*, *24*(01), 2450003.
3. Chen, C., Wang, X., Heidari, A. A., Yu, H., & Chen, H. (2021). Multi-threshold image segmentation of maize diseases based on elite comprehensive particle swarm optimization and otsu. *Frontiers in plant science*, *12*, 789911.
4. Yang, J., Ma, X., Guan, H., Yang, C., Zhang, Y., Li, G., ... & Lu, Y. (2024). A quality detection method of corn based on spectral technology and deep learning model. *Spectrochimica Acta Part A: Molecular and Biomolecular Spectroscopy*, *305*, 123472.
5. Soujanya, P. L., Sekhar, J. C., Yathish, K. R., Karjagi, C. G., Rao, K. S., Suby, S. B., ... & Rakshit, S. (2022). Leaf damage based phenotyping technique and its validation against fall armyworm, Spodoptera frugiperda (JE Smith), in maize. *Frontiers in Plant Science*, *13*, 906207.
6. Chimweta, M., Nyakudya, I. W., Jimu, L., & Bray Mashingaidze, A. (2020). Fall armyworm [Spodoptera frugiperda (JE Smith)] damage in maize: management options for flood-recession cropping smallholder farmers. *International journal of pest management*, *66*(2), 142-154.
7. Bernasconi, M. L., Turlings, T. C., Ambrosetti, L., Bassetti, P., & Dorn, S. (1998). Herbivore-induced emissions of maize volatiles repel the corn leaf aphid, Rhopalosiphum maidis. *Entomologia Experimentalis et Applicata*, *87*(2), 133-142.
8. Sytykiewicz, H., Łukasik, I., Goławska, S., & Chrzanowski, G. (2019). Aphid-triggered changes in oxidative damage markers of nucleic acids, proteins, and lipids in maize (Zea mays L.) seedlings. *International Journal of Molecular Sciences*, *20*(15), 3742.
9. Rehman, F., Khan, F. A., Anis, S. B., & Ansari, A. A. (2016). Plant defense response against grasshopper herbivory. *J. Entomol. Zool. Stud*, *4*, 184-190.
10. Meissle, M., Knecht, S., Waldburger, M., & Romeis, J. (2012). Sensitivity of the cereal leaf beetle Oulema melanopus (Coleoptera: Chrysomelidae) to Bt maize-expressed Cry3Bb1 and Cry1Ab. *Arthropod-Plant Interactions*, *6*, 203-211.
11. Abbas, A. H., Mirza, N. M., Qassir, S. A., & Abbas, L. H. (2020, February). Maize leaf images segmentation using color threshold and K-means clustering methods to identify the percentage of the affected areas. In *IOP Conference Series: Materials Science and Engineering* (Vol. 745, No. 1, p. 012048). IOP Publishing.

12. Lin, Z., Mu, S., Shi, A., Pang, C., & Sun, X. (2018). A novel method of maize leaf disease image identification based on a multichannel convolutional neural network. *Transactions of the ASABE*, *61*(5), 1461-1474.

13. Lv, M., Zhou, G., He, M., Chen, A., Zhang, W., & Hu, Y. (2020). Maize leaf disease identification based on feature enhancement and DMS-robust alexnet. *IEEE access*, *8*, 57952-57966.

14. Li, Z., Zhou, G., Hu, Y., Chen, A., Lu, C., He, M., ... & Wang, Y. (2022). Maize leaf disease identification based on WG-MARNet. *Plos one*, *17*(4), e0267650.

15. Zhang, X., Qiao, Y., Meng, F., Fan, C., & Zhang, M. (2018). Identification of maize leaf diseases using improved deep convolutional neural networks. *Ieee Access*, *6*, 30370-30377.

16. DeChant, C., Wiesner-Hanks, T., Chen, S., Stewart, E. L., Yosinski, J., Gore, M. A., ... & Lipson, H. (2017). Automated identification of northern leaf blight-infected maize plants from field imagery using deep learning. *Phytopathology*, *107*(11), 1426-1432.

17. Rai, C. K., & Pahuja, R. (2024). Northern maize leaf blight disease detection and segmentation using deep convolution neural networks. *Multimedia Tools and Applications*, *83*(7), 19415-19432.

18. Rabbi, R., Arefin, M. Y., Turna, I. F., & Zannat, Z. (2023). *Corn leaf disease detection using deep convolution neural network* (Doctoral dissertation, Brac University).

19. Xu, X., Wang, L., Shu, M., Liang, X., Ghafoor, A. Z., Liu, Y., ... & Zhu, J. (2022). Detection and counting of maize leaves based on two-stage deep learning with UAV-based RGB image. *Remote Sensing*, *14*(21), 5388.

20. Wu, J., Xiang, L., You, H., Tang, L., & Gai, J. (2024). Plant-Denoising-Net (PDN): A plant point cloud denoising network based on density gradient field learning. *ISPRS Journal of Photogrammetry and Remote Sensing*, *210*, 282-299.

21. Wu, X., Liu, Y., Xing, M., Yang, C., & Hong, S. (2024). Image segmentation for pest detection of crop leaves by improvement of regional convolutional neural network. *Scientific Reports*, *14*(1), 24160.

22. Yadav, A., & Dutta, M. K. (2018, February). An automated image processing method for segmentation and quantification of rust disease in maize leaves. In *2018 4th International Conference on Computational Intelligence & Communication Technology (CICT)* (pp. 1-5). IEEE.

23. Geng, T., Yu, H., Yuan, X., Ma, R., & Li, P. (2024). Research on segmentation method of maize seedling plant instances based on uav multispectral remote sensing images. *Plants*, *13*(13), 1842.

24. Bondre, S., & Patil, D. (2024). Crop disease identification segmentation algorithm based on Mask-RCNN. *Agronomy Journal*, *116*(3), 1088-1098.

25. Dalai, R., Dalai, N., & Senapati, K. K. (2024). A pest detection system for leaves through radial bi-symmetric divergence RCNN based segmentation approach. *Multimedia Tools and Applications*, 1-21.

26. Zhang, C., Zhou, J., Wang, H., Tan, T., Cui, M., Huang, Z., ... & Zhang, L. (2022). Multi-species individual tree segmentation and identification based on improved mask R-CNN and UAV imagery in mixed forests. *Remote Sensing*, *14*(4), 874.

27. Chisonga, C., Chipabika, G., Sohati, P. H., & Harrison, R. D. (2023). Understanding the impact of fall armyworm (Spodoptera frugiperda JE Smith) leaf damage on maize yields. *PLoS One*, *18*(6), e0279138.

28. Toepfer, S., Fallet, P., Kajuga, J., Bazagwira, D., Mukundwa, I. P., Szalai, M., & Turlings, T. C. (2021). Streamlining leaf damage rating scales for the fall armyworm on maize. *Journal of Pest Science*, *94*(4), 1075-1089.

29. Baudron, F., Zaman-Allah, M. A., Chaipa, I., Chari, N., & Chinwada, P. (2019). Understanding the factors influencing fall armyworm (Spodoptera frugiperda JE Smith) damage in African smallholder maize fields and quantifying its impact on yield. A case study in Eastern Zimbabwe. *Crop protection*, *120*, 141-150.

30. Tao, W., Wang, X., Xue, J. H., Su, W., Zhang, M., Yin, D., ... & Zhang, Y. (2022). Monitoring the damage of armyworm as a pest in summer corn by unmanned aerial vehicle imaging. *Pest Management Science*, *78*(6), 2265-2276.

31. Zhang, J., Huang, Y., Yuan, L., Yang, G., Chen, L., & Zhao, C. (2016). Using satellite multispectral imagery for damage mapping of armyworm (Spodoptera frugiperda) in maize at a regional scale. *Pest Management Science*, *72*(2), 335-348.

32. Ishengoma, F. S., Rai, I. A., & Said, R. N. (2021). Identification of maize leaves infected by fall armyworms using UAV-based imagery and convolutional neural networks. *Computers and Electronics in Agriculture*, *184*, 106124.

33. Chudzik, P., Mitchell, A., Alkaseem, M., Wu, Y., Fang, S., Hudaib, T., ... & Al-Diri, B. (2020). Mobile real-time grasshopper detection and data aggregation framework. *Scientific reports*, *10*(1), 1150.

34. Marvasti-Zadeh, S. M., Goodsman, D., Ray, N., & Erbilgin, N. (2023). Early detection of bark beetle attack using remote sensing and machine learning: A review. *ACM Computing Surveys*, *56*(4), 1-40.

35. Wei, S., Liu, X., McNeill, M. R., Wang, Y., Sun, W., Tu, X., ... & Zhang, R. (2023). Identification of spatial distribution and drivers for grasshopper populations based on geographic detectors. *Ecological Indicators*, *154*, 110500.

36. Sena Jr, D. G., Pinto, F. A. C., Queiroz, D. M., & Viana, P. A. (2003). Fall armyworm damaged maize plant identification using digital images. *Biosystems Engineering*, *85*(4), 449-454.

37. Kasoma, C., Shimelis, H., & Laing, M. D. (2021). Fall armyworm invasion in Africa: implications for maize production and breeding. *Journal of Crop Improvement*, *35*(1), 111-146.
38. Mutyambai, D. M., Niassy, S., Calatayud, P. A., & Subramanian, S. (2022). Agronomic factors influencing fall armyworm (Spodoptera frugiperda) infestation and damage and its co-occurrence with stemborers in maize cropping systems in Kenya. *Insects*, *13*(3), 266.
39. Neupane, S., Subedi, S., Neupane, P., & Shrestha, R. K. (2022). Screening of maize genotypes against maize leaf aphid [Rhopalosiphum maidis (Fitch)] under field condition at Chitwan, Nepal. *Journal of Nepal Agricultural Research Council*, *8*, 1-6.
40. Shrestha, S. (2014). Image denoising using new adaptive based median filters. *arXiv preprint arXiv:1410.2175*.